Dalton
Transactions

PAPER

Cite this: *Dalton Trans.*, 2018, **47**, 16674

Interplay between H-bonding and interpenetration in an aqueous copper(II)–aminoalcohol–pyromellitic acid system: self-assembly synthesis, structural features and catalysis†

Tiago A. Fernandes,[a] Marina V. Kirillova,*[a] Vânia André[a] and Alexander M. Kirillov *[a,b]

Received 21st July 2018,
Accepted 29th October 2018

DOI: 10.1039/c8dt02983k

rsc.li/dalton

Two new copper(II) coordination compounds, $[Cu(H_{1.5}mdea)_2]_2(H_2pma)$ (**1a**) and $[\{Cu_2(\mu\text{-}Hmdea)_2\}_2(\mu_4\text{-}pma)]_n\cdot 2nH_2O$ (**1b**), were self-assembled at different temperatures from the same multicomponent reaction system, comprising copper(II) nitrate, *N*-methyldiethanolamine (H_2mdea), pyromellitic acid (H_4pma), and potassium hydroxide. Products **1a** and **1b** were isolated as microcrystalline solids and fully characterized and their structures were established by single-crystal X-ray diffraction. Compound **1a** features the bis-aminoalcohol(ate) monocopper(II) units and H_2pma^{2-} anions that are multiply interconnected by strong H-bonds into a firm 2D H-bonded layer. Compound **1b** reveals the bis-aminoalcoholate dicopper(II) motifs that are interlinked by the μ_4-pma^{4-} spacers into a 3D + 3D interpenetrated metal–organic framework. From a topological perspective, both networks of **1a** and **1b** are uninodal and driven by similar 4-connected H_2pma^{2-} or pma^{4-} nodes, but result in distinct **sql** and **dia** topologies, respectively. Compound **1a** was applied as an efficient catalyst for two model cycloalkane functionalization reactions: (1) oxidation by H_2O_2 to form cyclic alcohols and ketones and (2) hydrocarboxylation by CO/H_2O and $S_2O_8{}^{2-}$ to form cycloalkanecarboxylic acids. The substrate scope, effects of various reaction parameters, selectivity and mechanistic features were also investigated.

Introduction

The synthesis of new metal–organic architectures assembled from different types of copper(II) cores has been of increased interest in recent years owing to a versatile coordination behavior of copper ions along with their promising redox, catalytic, and biological properties.[1–4] Synthetic approaches for copper(II) coordination compounds often rely on the self-assembly protocols, wherein various types of organic molecules are used as principal building blocks.[3–6] Among the great diversity of organic ligands, aminoalcohols and, in particular, ethanolamine derivatives represent an interesting class of compounds in view of their coordination versatility, flexibility, aqueous stability and solubility, as well as their commercial availability and low cost and due to the presence of different N,O-donor sites.[7] However, it is often difficult to assemble and crystallize copper(II)–aminoalcohol derivatives in an aqueous medium due to their high solubility; therefore, such synthetic approaches require the introduction of an additional, preferably anionic ligand that acts as a crystallization mediator or supporting block.[5–7] Carboxylic acids are very promising examples of such anionic ligands with a high affinity to copper(II) ions and rich coordination chemistry.[5,6]

Following the above discussion and our general interest in the aqueous medium self-assembly synthesis of diverse copper(II) cores and coordination polymers,[8] a primary objective of the present study has been to synthesize new metal–organic architectures from an aqueous three-component system, copper(II)–aminoalcohol–carboxylic acid. Herein, we have selected a simple diethanolamine derivative, *N*-methyldiethanolamine (H_2mdea), and an aromatic tetracarboxylic acid, pyromellitic acid (H_4pma), as principal building blocks (Scheme 1). Despite their recognized use in the design of diverse coordination compounds,[9–11] the combination of H_2mdea and H_4pma within one reaction system has not been explored and no Cu compounds containing both these blocks

---

[a] *Centro de Química Estrutural, Instituto Superior Técnico, Universidade de Lisboa, Av. Rovisco Pais, 1049-001 Lisboa, Portugal. E-mail: kirillova@tecnico.ulisboa.pt, kirillov@tecnico.ulisboa.pt; Tel: +351 218417178*

[b] *Peoples' Friendship University of Russia (RUDN University), Research Institute of Chemistry, 6 Miklukho-Maklaya st., Moscow, 117198, Russian Federation*

† Electronic supplementary information (ESI) available: Additional structural (Tables S1 and S2, Fig. S1–S3) and catalytic (Fig. S4–S7) data, as well as crystallographic CIF files for **1a** and **1b**. CCDC 1857110 and 1857111. For ESI and crystallographic data in CIF or other electronic format see DOI: 10.1039/c8dt02983k

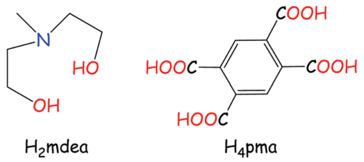

Scheme 1 Structural formulae of *N*-methyldiethanolamine and pyromellitic acid used as main building blocks.

have been documented, as confirmed by a search of the CSD (Cambridge Structural Database).[9]

Hence, in the present study we report an aqueous medium self-assembly synthesis, characterization, and structural and topological features of two new copper(II) coordination compounds, namely a discrete 0D derivative $[Cu(H_{1.5}mdea)_2]_2(H_2pma)$ (**1a**) and a 3D interpenetrated MOF $[\{Cu_2(\mu\text{-}Hmdea)_2\}_2(\mu_4\text{-}pma)]_n\cdot 2nH_2O$ (**1b**), which have been obtained at different temperatures from the same multicomponent reaction system. Besides, compound **1a** has been applied as an efficient homogeneous catalyst for the oxidative functionalization of cycloalkanes to give cyclic alcohols and ketones (oxidation reaction) or cycloalkanecarboxylic acids (hydrocarboxylation reaction). The selection of alkanes as substrates in catalytic tests has been governed by (1) the importance of these saturated hydrocarbons as abundant feedstocks,[12] (2) the industrial relevance of alkane oxidation products (*e.g.*, cyclohexanol and cyclohexanone are intermediates in nylon industry),[13] and (3) the presence of copper in the active sites of some enzymes, including the particulate methane monooxygenase that is capable of hydroxylating alkanes.[1,14]

Experimental

Materials and methods

All chemicals were obtained from commercial sources. Synthesis of **1a** and **1b** was carried out under an air atmosphere. Elemental (C, H, N) analyses were carried out by the Laboratory of Analyses of IST. Infrared spectra (4000–400 cm^{-1}) were recorded on a JASCO FT/IR-4100 equipment using KBr pellets (abbreviations: vs – very strong, s – strong, m – medium, w – weak, br – broad, sh – shoulder). ESI-MS(±) measurements were run on a LCQ Fleet mass spectrometer with an ESI source (Thermo Scientific), using $\sim 10^{-3}$ M solutions of **1a** or its model mixtures with HNO_3 and H_2O_2 in the aqueous medium. Gas chromatography (GC) analyses of the catalytic reaction mixtures were run on an Agilent Technologies 7820A series gas chromatograph (He as carrier gas) equipped with the FID detector and the BP20/SGE (30 m × 0.22 mm × 0.25 μm) capillary column.

Synthesis and characterization

$[Cu(H_{1.5}mdea)_2]_2(H_2pma)$ (1a). To an aqueous solution (10 mL) of $Cu(NO_3)_2\cdot 3H_2O$ (242 mg, 1 mmol), an aqueous solution of *N*-methyldiethanolamine (H_2mdea; 1 mL, 1 mmol) was added dropwise under constant stirring, followed by an addition of pyromellitic acid (H_4pma; 127 mg, 0.50 mmol) previously dissolved in an aqueous solution of KOH (3 mL, 3 mmol). The obtained mixture was stirred overnight at ambient temperature (~25 °C) and then filtered. The filtrate was left to slowly evaporate in a beaker at ambient temperature, resulting in the formation of blue crystals (including those suitable for single crystal X-ray diffraction) within 2 weeks. These were collected and dried in air to give compound **1a** in ~60% yield, based on copper(II) nitrate. Alternatively, compound **1a** can be generated by following the above procedure and using an excess of H_2mdea (0.573 mL, 5 mmol) instead of KOH. Compound **1a** is ionic and well soluble in H_2O ($S_{25\ °C} > 20$ mg mL^{-1}). Anal. calcd (%) for $\mathbf{1a}\cdot 6H_2O$: $C_{30}H_{66}Cu_2N_4O_{22}$ (MW 962): C 37.46, H 6.92, N 5.82; found C 37.42, H 6.77, N 6.03. FT-IR (KBr): 3519 (s br), 3456 (s br) and 3349 (s br) $\nu(OH/H_2O)$, 2991 (w), 2955 (w), 2914 (w), 2884 (w) $\nu(CH)$, 1902 (s br), 1624 (m sh), 1556 (s) $\nu_{as}(COO)$, 1481 (s), 1449 (w), 1402 (s sh), 1369 (vs br) $\nu_s(COO)$, 1321 (m), 1243 (w), 1133 (m), 1059 (s), 1025 (w), 997 (m), 904 (m), 890 (m), 844 (m), 795 (m), 763 (m), 665 (w), 618 (w), 582 (w), and 538 (m) cm^{-1}. ESI-MS(±) (H_2O), selected fragments: MS(+), *m*/*z*: 887 (5%) $[\{Cu(H_{1.5}mdea)_2\}_2(H_2pma) + 2H_2O + H]^+$, 734 (27%) $[Cu_2(Hmdea)_2(mdea)(H_4pma) + H]^+$, 555 (6%) $[Cu(Hmdea)_2(H_4pma) + H]^+$, 480 (98%) $[Cu_2(Hmdea)_3 + H]^+$, 300 (100%) $[Cu(Hmdea)(H_2mdea)]^+$; MS(−), *m*/*z*: 553 (5%) $[Cu(Hmdea)(H_2mdea)(H_2pma)]^-$, 253 (100%) $[(H_3pma)]^-$.

$[\{Cu_2(\mu\text{-}Hmdea)_2\}_2(\mu_4\text{-}pma)]_n\cdot 2nH_2O$ (1b). This compound was obtained by following the main procedure described for **1a** but performing an overnight reaction at higher temperature (~60 °C) and without stirring. This resulted in a deposition of blue microcrystals that were filtered to give **1b** as a blue solid in ~15% yield, based on copper(II) nitrate. The filtrate can be left to slowly evaporate in a beaker at r.t., resulting in the formation of a further crop of **1b** (~5% yield) along with **1a**. Compound **1b** is insoluble in water and organic solvents. Anal. calcd (%) for **1b**: $C_{30}H_{54}Cu_4N_4O_{18}$ (MW 1013): C 35.57, H 5.37, N 5.53; found C 35.29, H 5.48, N 5.41. FT-IR (KBr): 3302 (s br) $\nu(OH/H_2O)$, 2980 (w) and 2891 (w) $\nu(CH)$, 1636 (m), 1613 (m) and 1564 (vs) $\nu_{as}(COO)$, 1421 (m), 1384 (s) and 1333 (m) $\nu_s(COO)$, 1193 (w), 1140 (w), 1064 (s), 1017 (m), 901 (w), 896 (w), 754 (m), 667 (w) and 542 (w) cm^{-1}.

X-ray crystallography

Single crystals of **1a** and **1b** were mounted with Fomblin© in a cryoloop and the crystal data were collected on Bruker AXS-KAPPA APEX II and D8QUEST diffractometers with graphite-monochromated radiation (Mo Kα, $\lambda = 0.71073$ Å) and the X-ray generator operating at 50 kV and 30 mA. Data collection was monitored by the APEX2 program.[15] A correction for Lorentzian, polarization, and absorption effects was made using the SAINT and SADABS software.[15] SIR97 and/or SHELXS-97 programs[16,17] were applied for structure solution and SHELXL-97 was used for full matrix least-squares refinement on F^2;[17] these programs are in the WINGX-Version

1.80.05 package.[18] Non-H atoms were refined anisotropically. A full-matrix least-squares refinement was used for the non-H atoms with anisotropic thermal parameters. All the H atoms were inserted in idealized positions and allowed to refine in their parent carbon atom, except for the OH/H_2O moieties; these were located from the electron density map. The disorder model was applied to compound **1a**. PLATON software[19] was applied for the analysis of H-bond interactions. Crystal data and details of data collection for **1a** and **1b** are summarized in Table 1.

Topological analysis

Topological analysis of H-bonded (in **1a**) or metal–organic (in **1b**) networks was performed following the concept of the simplified underlying net.[20,21] Such underlying nets were generated by contracting discrete cations and anions (in **1a**) or bridging ligands (in **1b**) to the corresponding centroids, maintaining their connectivity *via* hydrogen or coordination bonds, respectively. In **1a**, only strong D–H⋯A hydrogen bonds were considered, wherein the H⋯A < 2.50 Å, D⋯A < 3.50 Å, and ∠(D–H⋯A) > 120°; D and A stand for donor and acceptor atoms.[20] The obtained underlying nets were then classified from the topological viewpoint.

Catalytic oxidation of alkanes

The catalytic reactions were performed in thermostated glass reactors equipped with a reflux condenser under vigorous stirring at 50 °C, under an air atmosphere, and using MeCN as the solvent (up to 5 mL total volume). In a typical test, the catalyst (10 μmol) and the GC internal standard ($MeNO_2$, 50 μL) were introduced into MeCN solution, followed by the addition of an acid promoter (typically 0.1 mmol, optional; used as a stock solution in MeCN) and an alkane substrate (2 mmol). The reaction was then initiated upon addition of H_2O_2 (50% in H_2O, 10 mmol) in one portion. The reaction progress was monitored by withdrawing small aliquots of the reaction mixtures after different periods of time. The aliquots were treated with PPh_3 for the reduction of remaining H_2O_2 and alkyl hydroperoxides that are typically formed as primary products in alkane oxidation.[22] The samples were analyzed by GC using nitromethane as an internal standard. Formation of alkyl hydroperoxides was confirmed by performing the GC analyses of selected samples two times, before and after the treatment with PPh_3 (Shul'pin's method).[22] GC peak assignment was made by comparison with chromatograms of authentic samples. Blank tests for all cycloalkane substrates tested confirmed that their oxidation does not proceed in the absence of the copper catalyst. Moreover, free ligands (H_2mdea, H_4pma) do not catalyze the oxidation of alkanes. Copper(II) nitrate as well as a mixture of $Cu(NO_3)_2$ with H_2mdea and H_4pma (*in situ* system resembling **1a**) results in significantly lower product yields (Fig. S4, ESI†) if compared with **1a**, thus confirming the need for a prior synthesis of the Cu(II) catalyst.[7a,8b]

Table 1 Crystal data and structure refinement details for **1a** and **1b**[a]

	1a	1b
Formula	$C_{30}H_{54}Cu_2N_4O_{16}$	$C_{15}H_{25}Cu_2N_2O_8\cdot H_2O$
Fw	853.87	506.49
Crystal form, color	Block, blue	Block, blue
Crystal size (mm)	0.18 × 0.08 × 0.06	0.08 × 0.05 × 0.03
Cryst. syst.	Triclinic	Tetragonal
Space group	$P\bar{1}$	$I4_1/acd$
a, Å	8.744(2)	13.8211(8)
b, Å	10.490(2)	13.8211(8)
c, Å	11.542(3)	41.437(2)
α, °	102.033(7)	90
β, °	91.299(12)	90
γ, °	100.042(9)	90
Z	1	16
T, K	298(2)	298(2)
D_c, g cm^{-3}	1.404	1.700
μ(Mo Kα), mm^{-1}	1.123	2.199
θ range (°)	2.370–30.738	2.304–27.131
Refl. Collected	57 135	26 048
Independent refl.	6150	2203
R_{int}	0.0376	0.0593
R_1 [a], wR_2 [b] [$I \geq 2\sigma(I)$]	0.0370, 0.1059	0.0325, 0.0702
GOF on F^2	1.062	1.048

[a] $R_1 = \sum||F_o| - |F_c||/\sum|F_o|$. [b] $wR_2 = [\sum[w(F_o^2 - F_c^2)^2]/\sum[w(F_o^2)^2]]^{1/2}$.

Catalytic hydrocarboxylation of cycloalkanes

In a typical hydrocarboxylation experiment, the reaction mixture was prepared as follows. The catalyst (10 μmol) was placed into a 20.0 mL stainless steel autoclave equipped with a Teflon-coated magnetic stirring bar, followed by the addition of $K_2S_2O_8$ (1.5 mmol), solvent (2.0 mL H_2O and 4.0 mL of MeCN; total solvent volume 6.0 mL), and cycloalkane substrate (1 mmol). The autoclave was closed and flushed with CO three times to remove the air, and finally pressurized with 20 atm of CO. CAUTION: Due to the toxicity of CO, all operations should be carried out in a well-ventilated hood! The reaction mixture was stirred for 4 h at 60 °C using a magnetic stirrer and an oil bath. Then, the autoclave was cooled in an ice bath, degassed, and opened, and the reaction mixture was transferred to a glass flask. Diethyl ether (9.0 mL) and 45 μL of cycloheptanone (typical GC internal standard) were added. For the cycloheptane hydrocarboxylation, cyclohexanone (45 μL) was used as a GC standard instead of cycloheptanone. The obtained mixture was vigorously stirred for 10 min, and the organic layer was analyzed by gas chromatography (internal standard method), revealing the formation of the corresponding monocarboxylic acids as major hydrocarboxylation products, along with cyclic alcohols and ketones as minor oxidation products. Attribution of peaks was made by comparison with chromatograms of authentic samples.

Results and discussion

Synthesis of 1a and 1b

A self-assembly reaction, at ~25 °C and in the aqueous medium, between copper(II) nitrate as a metal source, *N*-methyldiethanolamine (H_2mdea) as a principal building block, pyromellitic acid (H_4pma) as a crystallization mediator, and potassium hydroxide as a base, resulted in the generation of a novel coordination compound $[Cu(H_{1.5}mdea)_2]_2(H_2pma)$ (**1a**). This product is composed of two monocopper(II) bis-aminoalcohol(ate) $[Cu(H_2mdea)_2]^{2+}$ and $[Cu(Hmdea)_2]$ units and the H_2pma^{2-} anion, which are H-bonded into a 2D supramolecular network. However, a similar synthetic procedure performed at higher temperature (~60 °C) gave rise to a different product $[\{Cu_2(\mu\text{-}Hmdea)_2\}_2(\mu_4\text{-}pma)]_n\cdot 2nH_2O$ (**1b**), wherein the dicopper(II) bis-aminoalcoholate $[Cu_2(\mu\text{-}Hmdea)_2]^{2+}$ units are interlinked by the μ_4-pma^{4-} spacers into a 3D + 3D interpenetrated metal–organic framework. Compound **1b** typically crystallizes along with **1a** and the attempts to convert **1a** to **1b** in the aqueous medium at 50–60 °C were not successful. Phase purity of **1a** was confirmed by powder X-ray diffraction (Fig. S1†). Both products were isolated as blue, air-stable microcrystalline solids and were characterized by standard methods, including elemental analysis, IR spectroscopy, ESI-MS, single crystal X-ray diffraction and topological analysis.

Structural and topological description

$[Cu(H_{1.5}mdea)_2]_2(H_2pma)$ (1a). The structure of **1a** features a $[Cu(H_2mdea)_2]^{2+}$ cation, a neutral $[Cu(Hmdea)_2]$ unit, and an H_2pma^{2-} anion per formula unit (Fig. 1a). In both monocopper(II) blocks, the six-coordinate Cu1 and Cu2 atoms are located at an inversion center and display an octahedral $\{CuN_2O_4\}$ geometry. It is filled by a pair of H_2mdea (Cu1) or $Hmdea^-$ (Cu2) moieties that act as tridentate N,O_2-chelating ligands. The Cu–N [2.027(2)–2.038(3) Å] and Cu–O [2.031(3)–2.326(3) Å] distances are within typical values for such copper(II) derivatives.[10]

Although the H_2pma^{2-} moiety remained uncoordinated, there are very strong hydrogen bonding interactions between the H_2pma^{2-} and $[Cu(H_2mdea)_2]^{2+}$ and $[Cu(Hmdea)_2]$ units (Fig. 1a and Table S2†). In fact, the crystal packing pattern of **1a** reveals that each H_2pma^{2-} anion is bound by four pairs of H-bonds involving all pyromellitate COO/COOH groups and all O/OH functionalities of $H_2mdea/Hmdea^-$ ligands [O5–H⋯O1, 2.525(3) Å; O6A/B–H⋯O2, 2.608(10)/2.484(10) Å; O7–H⋯O7, 2.652(4) Å; O8–H⋯O4 2.483(3) Å]. As a result of these multiple interactions, a firm 2D H-bonded layer is generated (Fig. 1b). Topological classification of this layer was performed by analyzing its simplified underlying network (Fig. 1c), which is built from the 4-connected H_2pma^{2-} nodes and centroids of the 2-connected $[Cu(H_2mdea)_2]^{2+}$ and $[Cu(Hmdea)_2]$ linkers. This net can be classified as a uninodal 4-connected layer with the **sql** [Shubnikov tetragonal plane net] topology and a point symbol of $(4^4\cdot 6^2)$.[20]

$[\{Cu_2(\mu\text{-}Hmdea)_2\}_2(\mu_4\text{-}pma)]_n\cdot 2nH_2O$ (1b). Despite being self-assembled from the same reaction mixture as **1a**, the structure of **1b** is very different and shows a 3D + 3D interpenetrated metal–organic framework (Fig. 2). The asymmetric unit of **1b** comprises one Cu1 center, one μ-$Hmdea^-$ block, a quarter of μ_4-pma^{4-} spacer, and half of a H_2O molecule of crystallization. The Cu1 atoms and μ-$Hmdea^-$ blocks are arranged into the dicopper(II) bis-aminoalcoholate $[Cu_2(\mu\text{-}Hmdea)_2]^{2+}$ subunits with a rather short Cu1⋯Cu1 separation of 2.8559(6) Å (Fig. 2a). Within these Cu_2 subunits, the five-coordinate Cu1 centers display a distorted square-pyramid $\{CuNO_4\}$ environment. Herein, the basal sites are taken by the two symmetry generated O1 atoms and the N3 atom of μ-$Hmdea^-$ along with the O3 atom of μ_4-pma^{4-} [Cu1–O1 1.929(2), Cu1–N3 2.059(3), Cu1–O3 1.932(2) Å], whereas an apical site is occupied by the O2 atom (OH group) of the μ-$Hmdea^-$ moiety [Cu1–O2 2.393(2) Å]. The μ_4-pma^{4-} spacer acts as a 4-connected node and interlinks four $[Cu_2(\mu\text{-}Hmdea)_2]^{2+}$ subunits into an intricate 3D metal–organic framework (Fig. 2b).

From a topological perspective, a 3D MOF structure of **1b** is composed of the 4-connected μ_4-pma^{4-} nodes, 2-connected Cu1 centers, and 2-connected μ-$Hmdea^-$ linkers (Fig. 2c). Topological analysis of such a net reveals a uninodal 4-connected framework with the **dia** (Diamond) topology and a point symbol of (6^6).[20] A notable feature of this structure also concerns the presence of two independent 3D nets (Fig. 2d).

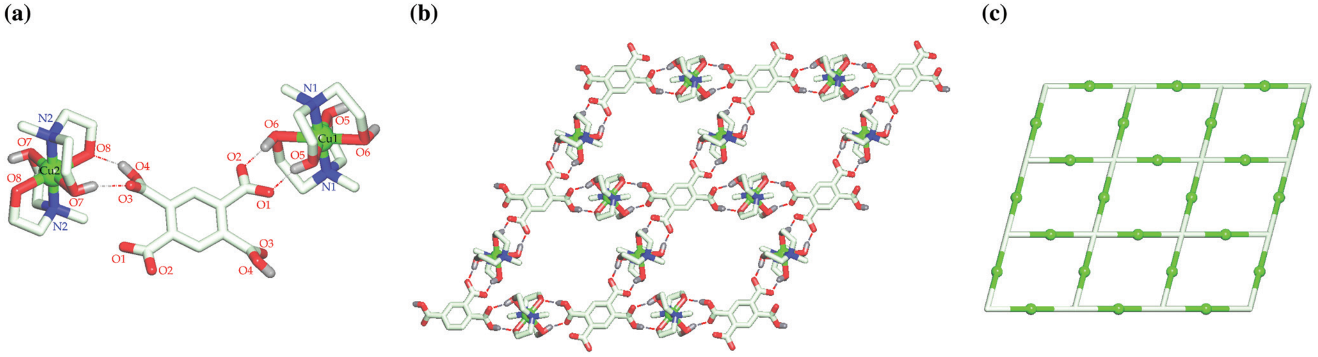

Fig. 1 Structural fragments of **1a**. (a) Molecular $[Cu(H_{1.5}mdea)_2]_2(H_2pma)$ unit with atom labelling and hydrogen bonds (red-gray dotted lines); CH hydrogen atoms were omitted for clarity. (b) 2D H-bonded layer; view along the *a* axis; Cu (green balls), N (blue), O (red), C (pale green), H (gray); H bonds are shown as red-gray dotted lines. (c) Topological representation of a 2D H-bonded net showing a uninodal 4-connected layer with the **sql** topology; centroids of 2-connected $[Cu(Hmdea)_2]$ and $[Cu(H_2mdea)_2]^{2+}$ units (green balls); centroids of 4-connected H_2pma^{2-} nodes (pale green), view along the *a* axis.

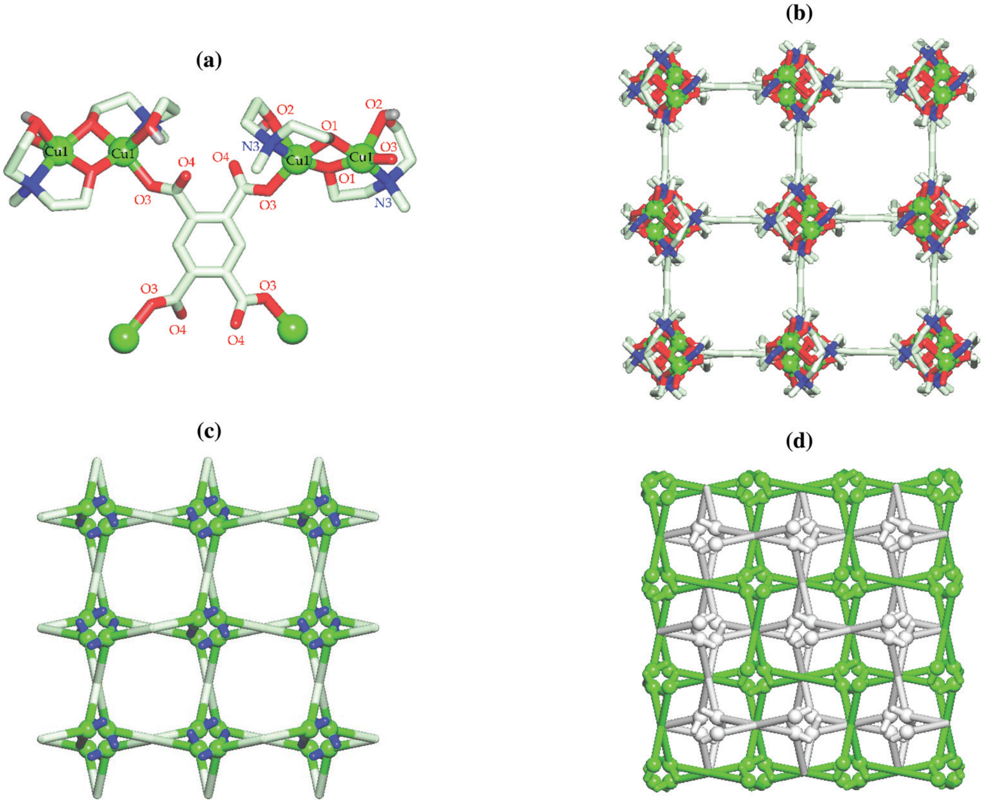

Fig. 2 Structural fragments of **1b**. (a) Interlinkage of two $[Cu_2(\mu\text{-}Hmdea)_2]^{2+}$ blocks and $\mu_4\text{-}pma^{4-}$ spacer; CH hydrogen atoms were omitted for clarity. (b) 3D metal–organic framework; view along the *c* axis; Cu (green balls), N (blue), O (red), C (pale green). (c) Topological representation of a 3D underlying net showing a uninodal 4-connected framework with the **dia** topology; 2-connected Cu centers (green balls), centroids of 4-connected $\mu_4\text{-}pma^{4-}$ nodes (pale green), centroids of 2-connected $\mu\text{-}Hmdea^{-}$ linkers (blue); view along the *c* axis. (d) Topological representation of two 3D + 3D interpenetrated nets represented by different colors (green and gray); Cu centers are shown as balls.

Analysis of their interpenetration discloses an extended 3D + 3D interpenetrated network (class IIa, *Z* = 2).

Mild catalytic oxidation of cycloalkanes

Despite being abundant hydrocarbon feedstocks, alkanes are very inert substrates and their oxidative functionalization under mild conditions continues to be a challenging research topic.[12] In industrially relevant processes, the oxidation of alkanes usually requires high temperatures and pressures, in addition to showing rather low product yields and selectivity. For example, an industrial oxidation of cyclohexane to cyclohexanol and cyclohexanone (nylon precursors) uses a homogeneous cobalt naphthenate catalyst, proceeds at ~150 °C, and requires multiple substrate recycling due to low overall product yields that do not exceed 5–10% (based on cyclohexane).[12,13]

Given the solubility of **1a** in the aqueous medium and following our interest in the search for new catalytic systems for mild alkane functionalization, we applied herein **1a** as a homogeneous catalyst for the mild oxidation of C_5–C_8 cycloalkanes by aqueous H_2O_2. The reaction proceeds at 50 °C and gives a mixture of the corresponding alcohols and ketones (Scheme 2a). The oxidation of all tested cycloalkanes proceeds with comparable reaction rates, although leading to different total product yields (Fig. 3 and S5†); hereinafter, all the yields are based on the cycloalkane substrate. Cyclooctane and cycloheptane appear to be more reactive substrates leading to total product yields of ~22–23%, followed by cyclohexane (~18%) and cyclopentane (~10%).

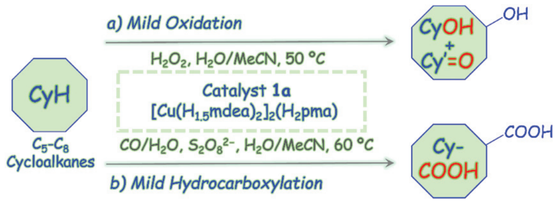

Scheme 2 Mild oxidation (a) and hydrocarboxylation (b) of C_5–C_8 cycloalkanes (CyH) to give the corresponding cyclic alcohols (CyOH) and ketones (Cy′=O), or cycloalkanecarboxylic acids (CyCOOH).

Oxidation of cycloalkanes in the presence of **1a** is promoted by a catalytic amount of acid. We studied the effect of different acid promoters on the oxidation of C_6H_{12} (Fig. 4). In the presence of HCl, the oxidation proceeds very quickly and results in ~17% total yield after 10 min; further increase of reaction time leads to product consumption due to overoxidation. Although

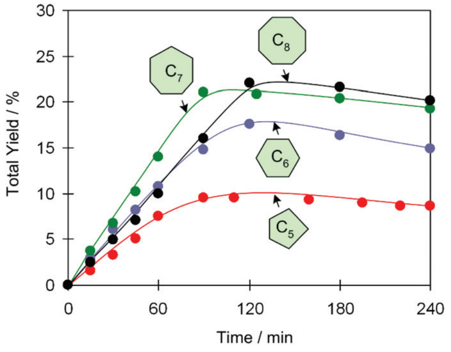

Fig. 3 Oxidation of C_5–C_8 cycloalkanes (total yield of alcohol and ketone *vs.* time) with H_2O_2 catalyzed by **1a** in the presence of TFA promoter. Reaction conditions: Catalyst **1a** (0.01 mmol), TFA (0.1 mmol), cycloalkane (2 mmol), H_2O_2 (50% in H_2O, 10 mmol), CH_3CN (up to 5.0 mL total volume), and 50 °C.

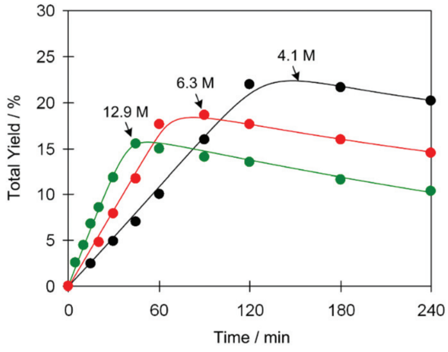

Fig. 5 Effect of the H_2O amount on the total product yield in the cyclooctane oxidation with H_2O_2 catalyzed by **1a**/TFA. Reaction conditions: Catalyst **1a** (0.01 mmol), TFA (0.1 mmol), C_8H_{16} (2 mmol), H_2O_2 (50% in H_2O, 10 mmol), added H_2O (up to 0.8 mL), CH_3CN (up to 5.0 mL total volume), and 50 °C.

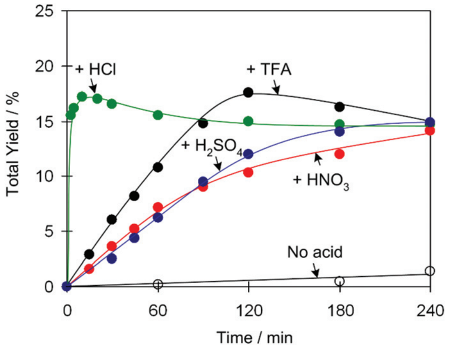

Fig. 4 Effect of the type of acid promoter on the total product yield in the cyclohexane oxidation with H_2O_2 catalyzed by **1a**. Reaction conditions: Catalyst **1a** (0.01 mmol), acid promoter (0.1 mmol), C_6H_{12} (2 mmol), H_2O_2 (50% in H_2O, 10 mmol), CH_3CN (up to 5.0 mL total volume), and 50 °C.

such an accelerating effect of HCl is not yet clearly understood, it can be associated with an ability of chloride anions to stabilize a Cu(I) oxidation state (or Cu–peroxo intermediates) *via* the formation of copper aminoalcohol(ate) moieties bearing terminal or bridging Cl^- ligands.[7a]

A slightly better yield of 18% is achieved after 120 min in the presence of trifluoroacetic acid (TFA) as a promoter. Nitric acid and sulfuric acid also promote the oxidation of cyclohexane, although in these cases the reactions are slower and lead to ~15% yields after 240 min. TFA was thus selected as a promoter for studying the effects of other reaction parameters.

The influence of the TFA amount on the oxidation of cyclooctane catalyzed by **1a** was also investigated (Fig. S6, ESI†). The increase of the TFA amount from 0 to 5 equivalents relatively to the catalyst leads to a gradual growth of both the total product yield and an initial reaction rate, W_0. The latter reveals an s-shape dependence on the TFA concentration (Fig. S6b†). Higher TFA amounts (10 or 20 equivalents *vs.* catalyst) almost do not affect the initial reaction rate, but result in superior product yields (*e.g.*, 22% at 10 equivalents of TFA).

We also studied the effect of the catalyst amount and observed a linear dependence of the initial reaction rate W_0 on the catalyst concentration (Fig. S7, ESI†) in the cyclooctane oxidation catalyzed by the **1a**/TFA system. This behavior indicates the first-order reaction kinetics, which supports an involvement of one type of Cu-containing species in the rate-limiting catalytic step. The increase of the catalyst concentration from 0.5 to 2.0 mM also results in a linear growth of the maximum product yield (up to 22%).

An interesting accelerating effect of water on the initial reaction rate of cyclooctane oxidation was observed in the **1a**/TFA system (Fig. 5). The W_0 increases on increasing the water concentration in the system from 4.1 M (corresponds to the amount of H_2O in 50% aqueous H_2O_2) to 12.9 M (after introduction of an additional amount of water to the reaction mixture). However, a higher water amount in the system leads to a drop of the total product yield from 22 to 16%, respectively. This can be related to a lower solubility of cyclooctane in the reaction mixture at a higher content of water. Thus, we can propose an involvement of water in the rate limiting step of catalytic generation of hydroxyl radicals.[8]

To evaluate the stability of the catalytic system and elucidate some mechanistic aspects, we also performed a stepwise oxidation of cyclooctane (Fig. 6). Since the C_8H_{16} oxidation in the presence of **1**/TFA requires 120 min to achieve the maximum product yield (Fig. 3), after this period of time we introduced a new portion of cyclooctane and H_2O_2 into the reaction medium without an addition of a new loading of catalyst. The oxidation restarted even with a higher reaction rate. One more addition of both the oxidant and substrate after 4 h again allows continuing the cyclooctane oxidation. This shows that the catalytically active Cu species is stable in the reaction solution and alive for a long time. The oxidation reaction ends due to the consumption of H_2O_2, since the introduction of only the substrate (without an addition of H_2O_2) does not allow to restart the reaction.

To gain additional insight into the nature of catalytically active species, we studied the aqueous solutions of **1a** (**1a**/H^+)

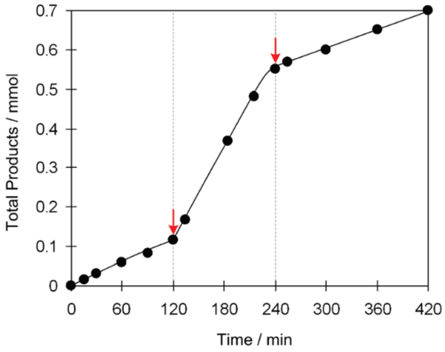

Fig. 6 Stepwise oxidation of cyclooctane with H_2O_2 catalyzed by **1a**/TFA. On each step (at 120 and 240 min) a new portion of C_8H_{16} (1 mmol) and H_2O_2 (5 mmol) was added. Reaction conditions: Catalyst **1a** (0.01 mmol), TFA (0.1 mmol), C_8H_{16} (1 mmol), H_2O_2 (50% in H_2O, 5 mmol), CH_3CN (up to 5.0 mL total volume), and 50 °C.

and **1a**/H^+/H_2O_2 by ESI-MS(±), using the conditions typical to those of catalytic tests. The following main fragments can be observed in the MS(+) spectra of **1a** (**1a**/H^+): $[\{Cu(H_{1.5}mdea)_2\}_2(H_2pma) + 2H_2O + H]^+$ (*m*/*z* 887), $[Cu_2(Hmdea)_2(mdea)(H_4pma) + H]^+$ (*m*/*z* 734) $[Cu(Hmdea)_2(H_4pma) + H]^+$ (*m*/*z* 555), $[Cu_2(Hmdea)_3 + H]^+$ (*m*/*z* 480), and $[Cu(Hmdea)(H_2mdea)]^+$ (*m*/*z* 300). Apart from expected monocopper bis-aminoalcohol(ate) species, there are also heavier fragments due to their aggregation and interaction with a pyromellitate anion. A characteristic molecular ion peak, $[Cu(Hmdea)(H_2mdea)(H_2pma)]^-$ (*m*/*z* 553), was also observed with the expected isotopic distribution pattern in the MS(−) mode, along with the $[(H_3pma)]^-$ (*m*/*z* 253) anion. The ESI-MS plots of a model **1a**/H^+/H_2O_2 solution also show some of the above-mentioned fragments (*e.g.*, $[Cu(Hmdea)(H_2mdea)(H_2pma)]^-$ (*m*/*z* 553), in addition to new intense peaks that are particularly pronounced in a negative mode. These are the $[Cu(Hmdea)_2(H_3pma)_2 - 2(COOH)]^-$ (*m*/*z* 719) and $[Cu(Hmdea)_2(H_2pma) - COOH]^-$ (*m*/*z* 507) fragments, generated as a result of ESI- and H_2O_2-induced decarboxylation of pyromellitate anions. This observation, along with a catalyst stability study (Fig. 6), suggests that the monocopper bis-aminoalcohol(ate) units and respective adducts with pyromellitate anions may represent the catalytically active species in the present system.

Selectivity and mechanistic features in mild alkane oxidation

To obtain further mechanistic evidence, we performed the oxidation of linear and branched alkanes in order to determine various types of selectivity parameters (Table 2). The oxidation of linear alkanes (*n*-pentane, *n*-hexane, *n*-heptane, *n*-octane) results in regioselectivity C(1) : C(2) : C(3) : (C4) parameters of 1 : 13 : 14, 1 : 8 : 13, 1 : 9 : 12 : 16, and 1 : 17 : 24 : 23, respectively; these also reveal some preference to the oxidation at the internal C(3) or C(4) secondary carbon atom of the hydrocarbon chain. For the oxidation of methylcyclohexane, a normalized bond selectivity 1° : 2° : 3° parameter of 1 : 9 : 36 was obtained, suggesting that the tertiary C atom is oxidized with a considerable preference over to the secondary C atoms. In the oxidation of adamantane, the 3°/2° parameter of 3.8 is less pronounced if compared to the respective ratio (1° : 2° : 3° of 1 : 9 : 36) in the oxidation of methylcyclohexane. The oxidations of both *cis*- or *trans*-1,2-dimethylcyclohexanes proceed non-stereoselectively, as attested by the *trans*/*cis* ratios of 0.7 between the generated isomeric tertiary alcohols with the mutual *trans* and *cis* orientation of the CH_3 groups. Partial inversion of the configuration was detected and the *cis* isomers are the predominant products in the oxidation of both *cis*- and *trans*-1,2-dimethylcyclohexane.

Table 2 Different selectivity parameters in the oxidation of linear and branched alkanes catalyzed by **1a**[a]

Selectivity (substrate)	Selectivity value
Regioselectivity	
C(1) : C(2) : C(3)[b] (*n*-C_5H_{12})	1 : 13 : 14
C(1) : C(2) : C(3)[b] (*n*-C_6H_{14})	1 : 8 : 13
C(1) : C(2) : C(3) : C(4)[b] (*n*-C_7H_{16})	1 : 9 : 12 : 16
Bond selectivity	
1° : 2° : 3° (methylcyclohexane)[c]	1 : 9 : 36
3°/2° (adamantane)[d]	3.8
Stereoselectivity	
trans/*cis* (*cis*-Dimethylcyclohexane)[e]	0.7
trans/*cis* (*trans*-Dimethylcyclohexane)[e]	0.7

[a] Reaction conditions: Catalyst **1a** (0.005 mmol), TFA (0.05 mmol), alkane (1 mmol), H_2O_2 (50% in H_2O, 5 mmol), MeCN up to 2.5 mL total volume, 2 h, and 50 °C. All selectivity parameters were calculated based on the ratios of isomeric alcohols. Normalization of the values was performed by taking into account the number of hydrogen atoms at each carbon atom. [b] Parameters C(1) : C(2) : C(3) : (C(4)) are the relative reactivities of H atoms at C(1), C(2), C(3), and C(4) (optional) carbon atoms of the *n*-alkane chain. [c] Parameters 1° : 2° : 3° are the relative normalized reactivities of the hydrogen atoms at primary, secondary and tertiary carbon atoms of methylcyclohexane. [d] Parameters 3°/2° are the relative normalized reactivities of the hydrogen atoms at tertiary and secondary carbon atoms of adamantane, determined as the ratio of the formed tertiary and secondary alcohol isomers. [e] Parameter *trans*/*cis* is determined as the ratio of the formed tertiary alcohol isomers with mutual *trans* and *cis* orientation of the methyl groups.

Analysis of all these selectivity patterns and prior literature background[8,22,23] suggest that the present reactions involve powerful and indiscriminate oxidizing species, namely the $HO^•$ radicals that are formed as a result of the interaction of H_2O_2 with the copper catalyst. The proposed reaction mechanism thus relies on hydroxyl radicals that abstract the H atom from an alkane substrate (RH) to give alkyl radicals ($R^•$). These couple with O_2 (*e.g.*, formed from H_2O_2 or from air) to furnish the alkyl peroxo ($ROO^•$) radicals, which then give rise to ROO^- (and a regeneration of the Cu^{II} catalyst) and then alkyl hydroperoxides (ROOH) as primary intermediate products. The latter were detected by GC following a method of Shul'pin;[22] ROOH then decompose to furnish the corresponding alcohols and ketones as final oxidation products.

Catalytic hydrocarboxylation of cycloalkanes

Apart from the mild alkane oxidation reactions, we also investigated the catalytic behavior of **1a** in the hydrocarboxylation of cycloalkanes. This transformation consists of the reaction of a C_n cycloalkane with carbon monoxide (carbonyl source) and water (hydroxyl source) to form directly C_{n+1} cycloalkanecarboxylic acid. The reaction requires the presence of a potent peroxodisulfate oxidant (*e.g.*, $K_2S_2O_8$) and proceeds at 60 °C in the water–acetonitrile medium (Scheme 2b).

Compound **1a** acts as an efficient catalyst toward the hydrocarboxylation of cyclopentane, cyclohexane, cycloheptane, and cyclooctane with overall product yields up to 45% based on cycloalkane (Table 3). The highest activity was observed for the cyclohexane substrate, leading to 43% yield of $C_6H_{11}COOH$, followed by cyclopentane (30% of C_5H_9COOH) and cycloheptane (23% of $C_7H_{13}COOH$). The yield of carboxylic acid ($C_8H_{15}COOH$) drops to 9% when using cyclooctane as the substrate. The corresponding cyclic ketones and alcohols are also formed as by-products of a competing oxidation reaction. The total yield of oxygenates (ketone is formed predominantly to alcohol) increases with the hydrocarbon size, namely from 0.5% for C_5H_{10} to 12.8% for C_8H_{16}.

As in the case of cycloalkane oxidation, there is strong evidence that the present type of hydrocarboxylation proceeds *via* a free-radical mechanism.[7a,24] In fact, sulfate radical anions ($SO_4^{\bullet-}$) are the key species formed from the $S_2O_8^{2-}$ oxidant through the Cu-assisted and/or temperature-assisted oxidant activation processes. Then, $SO_4^{\bullet-}$ react with a cycloalkane (RH) to abstract an H atom and generate cycloalkyl radicals ($R^\bullet$), followed by their reaction with CO to give cycloacyl radicals ($RCO^\bullet$). The latter undergo oxidation by Cu^{II} to form cycloacyl cations (RCO^+) which were then hydrolyzed by water to give cycloalkanecarboxylic acids (RCOOH) as main hydrocarboxylation products.[24]

Table 3 Single-pot hydrocarboxylation of C_n (n = 5–8) cycloalkanes into the corresponding C_{n+1} cycloalkanecarboxylic acids catalyzed by **1a**[a]

		Product yield[b], %			
Entry	Cycloalkane	Cycloalkane-carboxylic acid	Ketone	Alcohol	Total[c]
1		29.7	0.5	Traces	30.2
2	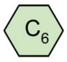	42.6	1.8	0.5	44.9
3		22.8	7.0	2.2	32.0
4	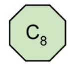	8.8	12.8	6.1	27.7

[a] Cyclic ketones and alcohols are also formed as by-products of cycloalkane oxidation. Reaction conditions: Catalyst **1a** (0.01 mmol), cycloalkane (1 mmol), p(CO) (20 atm), $K_2S_2O_8$ (1.5 mmol), H_2O (2.0 mL)/MeCN (4.0 mL), 60 °C, 4 h in an autoclave (20 mL capacity). [b] (Moles of product/mole of cycloalkane) × 100%. [c] Yield of all products.

Conclusions

In the present work, we investigated the self-assembly synthesis of copper(II) coordination compounds from a multicomponent aqueous system composed of Cu(II) nitrate, *N*-methyldiethanolamine, pyromellitic acid and a base (KOH). Interestingly, two distinct products can be generated depending on the reaction temperature. At 25 °C, a discrete 0D compound $[Cu(H_{1.5}mdea)_2]_2(H_2pma)$ (**1a**) is formed as a sole product in a good yield. However, at a higher reaction temperature of 60 °C, a 3D interpenetrated MOF $[\{Cu_2(\mu\text{-Hmdea})_2\}_2(\mu_4\text{-pma})]_n{\cdot}2nH_2O$ (**1b**) is generated as a minor product along with **1a**. The analysis of crystal structures, packing patterns, and topological features of **1a** and **1b** suggests that there is an interplay between the H-bonding interactions and interpenetration during the crystallization of these products. In fact, both structures are driven by the H_2pma^{2-}/pma^{4-} blocks that act as similar 4-connected nodes and lead to the extension of **1a** into a 2D H-bonded layer or the generation of an intricate interpenetrated 3D + 3D metal–organic network in **1b**. The 2D and 3D underlying nets in **1a** and **1b** were topologically classified revealing the **sql** and **dia** topologies, respectively. Hence, the present study also contributes to intensive research on the assembly of various interpenetrated metal–organic architectures.[25,26]

Given good solubility of **1a** in the aqueous medium, this compound was also tested as a homogeneous catalyst for the mild oxidative functionalization of C_5–C_8 cycloalkanes (C_5H_{10}, C_6H_{12}, C_7H_{14}, and C_8H_{16}) and two model oxidation and hydrocarboxylation reactions were explored. Hence, compound **1a** catalyzes the oxidation of cycloalkanes by H_2O_2 to form a mixture of the respective cyclic alcohols and ketones. Interestingly, the product yields grow on increasing the carbon ring size in the homologous series of cycloalkane substrates, which can be associated with an increased stability of cycloalkyl radicals having more carbon atoms within the ring.

Besides, the catalytic efficiency of **1a** in cycloalkane oxidation depends on the type and amount of an acid promoter and the quantity of water in the system. Furthermore, **1a** also catalyzes the mild hydrocarboxylation of cycloalkanes, by CO/H_2O and $S_2O_8^{2-}$, to give the corresponding cycloalkanecarboxylic acids. In both oxidation and hydrocarboxylation processes, the obtained total product yields (up to 45%, based on cycloalkane) are considered high in the area of alkane functionalization, especially if taking into account an intrinsic inertness of such hydrocarbons and rather mild reaction conditions (*e.g.*, 50–60 °C temperature, aqueous medium).[12,13,22–24,27,28] Furthermore, the total product yields achieved herein are better or comparable to those commonly observed in the oxidative functionalization of cycloalkanes catalyzed by other Cu-containing systems containing aminoalcohol(ate) and carboxylate blocks.[7a,8,24b]

The research on exploring such a type of multicomponent copper(II)–aminoalcohol–carboxylic acid system for the self-assembly generation of diverse copper cores and metal–organic frameworks with notable structural, topological, and functional characteristics is underway in our laboratory.

Conflicts of interest

There are no conflicts to declare.

Acknowledgements

This work was supported by the Foundation for Science and Technology (FCT) and Portugal 2020 (projects IF/01395/2013/CP1163/CT005, CEECIND/03708/2017, UID/QUI/00100/2013, LISBOA-01-0145-FEDER-029697, and REM2013). The publication was also prepared with the support of the RUDN University Program 5-100. We thank Ms S. Dias for experimental assistance, Dr M. C. Oliveira and Ms A. Dias for ESI-MS (±) measurements. AMK also acknowledges the EU COST Action CA15106 (CHAOS).

Notes and references

1 (*a*) *Bioinorganic Chemistry of Copper*, ed. K. D. Karlin and Z. Tyeklar, Springer, Berlin, 2012; (*b*) *Copper-Oxygen Chemistry*, ed. S. Itoh and S. Rokita, Wiley, New York, 2011.

2 (*a*) L. Pandolfo and C. Pettinari, *CrystEngComm*, 2017, **19**, 1701; (*b*) C. Pettinari, A. Tabacaru and S. Galli, *Coord. Chem. Rev.*, 2016, **307**, 1.

3 (*a*) M. I. H. Mohideen, B. Xiao, P. S. Wheatley, A. C. McKinlay, Y. Li, A. M. Z. Slawin, D. W. Aldous, N. F. Cessford, T. Duren, X. B. Zhao, R. Gill, K. M. Thomas, J. M. Griffin, S. E. Ashbrook and R. E. Morris, *Nat. Chem.*, 2011, **3**, 304; (*b*) M. I. Mohideen, P. K. Allan, K. W. Chapman, J. A. Hriljac and R. E. Morris, *Dalton Trans.*, 2014, **43**, 10438.

4 (*a*) E. Loukopoulos, M. Kallitsakis, N. Tsoureas, A. Abdul-Sada, N. F. Chilton, I. N. Lykakis and G. E. Kostakis, *Inorg. Chem.*, 2017, **56**, 4898; (*b*) E. Loukopoulos, A. Michail and G. E. Kostakis, *Crystals*, 2018, **8**, 47; (*c*) K. A. D. F. Castro, F. Figueira, R. F. Mendes, J. A. S. Cavaleiro, M. G. P. M. S. Neves, M. M. Q. Simões, F. A. A. Paz, J. P. C. Tomé and S. Nakagaki, *ChemCatChem*, 2017, **9**, 2939; (*d*) Ł. Jaremko, A. M. Kirillov, P. Smoleński and A. J. L. Pombeiro, *Cryst. Growth Des.*, 2009, **9**, 3006; (*e*) R. Thenarukandiyil, C. Dutta and J. Choudhury, *Chem. – Eur. J.*, 2017, **23**, 15529.

5 For selected books, see: (*a*) *The Chemistry of Metal-Organic Frameworks, 2 Volume Set: Synthesis, Characterization, and Applications*, ed. S. Kaskel, John Wiley & Sons, 2016; (*b*) *Metal-Organic Framework Materials*, ed. L. R. MacGillivray and C. M. Lukehart, John Wiley & Sons, Chichester, U.K., 2014.

6 (*a*) J. Y. Lu, *Coord. Chem. Rev.*, 2003, **246**, 327; (*b*) A. Y. Robin and K. M. Fromm, *Coord. Chem. Rev.*, 2006, **250**, 2127.

7 For reviews, see: (*a*) A. M. Kirillov, M. V. Kirillova and A. J. L. Pombeiro, *Coord. Chem. Rev.*, 2012, **256**, 2741; (*b*) A. Singh and R. C. Mehrotra, *Coord. Chem. Rev.*, 2004, **248**, 101; (*c*) J. G. Verkade, *Acc. Chem. Res.*, 1993, **26**, 483.

8 (*a*) T. A. Fernandes, C. I. M. Santos, V. André, J. Kłak, M. V. Kirillova and A. M. Kirillov, *Inorg. Chem.*, 2016, **55**, 125; (*b*) S. S. P. Dias, M. V. Kirillova, V. André, J. Kłak and A. M. Kirillov, *Inorg. Chem. Front.*, 2015, **2**, 525; (*c*) S. S. P. Dias, M. V. Kirillova, V. André, J. Kłak and A. M. Kirillov, *Inorg. Chem.*, 2015, **54**, 5204.

9 See the Cambridge Structural Database: C. R. Groom, I. J. Bruno, M. P. Lightfoot and S. C. Ward, *Acta Crystallogr., Sect. B: Struct. Sci., Cryst. Eng. Mater.*, 2016, **72**, 171.

10 For selected examples of Cu/H_2mdea derivatives, see: (*a*) F. Sama, A. K. Dhara, M. N. Akhtar, Y.-C. Chen, M.-L. Tong, I. A. Ansari, M. Raizada, M. Ahmad, M. Shahid and Z. A. Siddiqi, *Dalton Trans.*, 2017, **46**, 9801; (*b*) S. S. P. Dias, V. Andre, J. Klak, M. T. Duarte and A. M. Kirillov, *Cryst. Growth Des.*, 2014, **14**, 3398; (*c*) G. Xu, X. He, J. Lv, Z. Zhou, Z. Du and Y. Xie, *Cryst. Growth Des.*, 2012, **12**, 3619.

11 For selected examples of Cu/H_4pma derivatives, see: (*a*) T. A. Beard, J. Z. Travis and R. L. LaDuca, *Inorg. Chim. Acta*, 2017, **459**, 143; (*b*) A. M. Fidelli, V. G. Kessler, A. Escuer and G. S. Papaefstathiou, *CrystEngComm*, 2017, **19**, 4355; (*c*) T. A. Fernandes, C. I. M. Santos, V. Andre, S. S. P. Dias, M. V. Kirillova and A. M. Kirillov, *Catal. Sci. Technol.*, 2016, **6**, 4584.

12 (*a*) G. A. Olah, A. Molnar and G. K. Surya Prakash, *Hydrocarbon Chemistry*, Wiley, 2017; (*b*) A. E. Shilov and G. B. Shul'pin, *Activation and Catalytic Reactions of Saturated Hydrocarbons in the Presence of Metal Complexes*, Kluwer Acad. Publ., Dordrecht, 2000.

13 U. Schuchardt, D. Cardoso, R. Sercheli, R. Pereira, R. S. da Cruz, M. C. Guerreiro, D. Mandelli, E. V. Spinace and E. L. Pires, *Appl. Catal., A*, 2001, **211**, 1.

14 S. Sirajuddin and A. C. Rosenzweig, *Biochemistry*, 2015, **54**, 2283.

15 *Bruker Analytical Systems*, Madison, WI, 2005.

16 A. Altomare, M. C. Burla, M. Camalli, G. L. Cascarano, C. Giacovazzo, A. Guagliardi, A. G. Moliterni, G. Polidori and R. Spagna, *J. Appl. Crystallogr.*, 1999, **32**, 115.

17 G. M. Sheldrick, *Acta Crystallogr., Sect. A: Found. Crystallogr.*, 2008, **64**, 112.

18 L. J. Farrugia, *J. Appl. Crystallogr.*, 1999, **32**, 837.

19 A. L. Spek, *Acta Crystallogr., Sect. D: Biol. Crystallogr.*, 2009, **65**, 148.

20 (*a*) V. A. Blatov, *IUCr Comp. Comm. Newslett*, 2006, **7**, 4; (*b*) V. A. Blatov, A. P. Shevchenko and D. M. Proserpio, *Cryst. Growth Des.*, 2014, **14**, 3576.

21 (*a*) M. O'Keeffe and O. M. Yaghi, *Chem. Rev.*, 2012, **112**, 675; (*b*) M. Li, D. Li, M. O'Keeffe and O. M. Yaghi, *Chem. Rev.*, 2014, **114**, 1343.

22 (*a*) G. B. Shul'pin, *Catalysts*, 2016, **6**, 50; (*b*) G. B. Shul'pin, *J. Mol. Catal. A: Chem.*, 2002, **189**, 39; (*c*) G. B. Shul'pin, *C. R. Chim.*, 2003, **6**, 163; (*d*) G. B. Shul'pin, *Mini-Rev. Org. Chem.*, 2009, **6**, 95.

23 (*a*) G. B. Shul'pin, *Dalton Trans.*, 2013, **42**, 12794; (*b*) G. B. Shul'pin, *Org. Biomol. Chem.*, 2010, **8**, 4217.

24 (*a*) K. D. Demadis, Z. Anagnostou, A. Panera, G. Mezei, M. V. Kirillova and A. M. Kirillov, *RSC Adv.*, 2017, **7**, 17788; (*b*) T. A. Fernandes, V. André, A. M. Kirillov and M. V. Kirillova, *J. Mol. Catal. A: Chem.*, 2017, **426**, 357; (*c*) M. V. Kirillova, A. M. Kirillov, M. L. Kuznetsov, J. A. L. Silva, J. J. R. Frausto da Silva and A. J. L. Pombeiro, *Chem. Commun.*, 2009, 2353.

25 For selected seminal reviews on interpenetrated nets, see: (*a*) H.-L. Jiang, T. A. Makal and H.-C. Zhou, *Coord. Chem. Rev.*, 2013, **257**, 2232; (*b*) V. A. Blatov, L. Carlucci, G. Ciani and D. M. Proserpio, *CrystEngComm*, 2004, **6**, 377; (*c*) L. Carlucci, G. Ciani and D. M. Proserpio, *Coord. Chem. Rev.*, 2003, **246**, 247; (*d*) S. R. Batten and R. Robson, *Angew. Chem., Int. Ed.*, 1998, **37**, 1460.

26 (*a*) S. A. Sotnik, R. A. Polunin, M. A. Kiskin, A. M. Kirillov, V. N. Dorofeeva, K. S. Gavrilenko, I. L. Eremenko, V. M. Novotortseva and S. V. Kolotilov, *Inorg. Chem.*, 2015, **54**, 5169; (*b*) W. Huang, F. Pan, Y. Liu, S. Huang, Y. Li, J. Yong, Y. Li, A. M. Kirillov and D. Wu, *Inorg. Chem.*, 2017, **56**, 6362.

27 (*a*) M. M. Levitsky, A. I. Yalymov, A. N. Kulakova, A. A. Petrova and A. N. Bilyachenko, *J. Mol. Catal. A: Chem.*, 2017, **426**, 297; (*b*) A. A. Shteinman, *J. Mol. Catal. A: Chem.*, 2017, **426**, 305.

28 K. M. Mantovani, K. C. M. Westrup, R. M. da Silva Junior, S. Jaerger, F. Wypych and S. Nakagaki, *Dalton Trans.*, 2018, **47**, 3068.